

First-principles computation of structural, elastic and magnetic properties of Ni₂FeGa across the martensitic transformation

This article has been downloaded from IOPscience. Please scroll down to see the full text article.

2013 J. Phys.: Condens. Matter 25 025502

(<http://iopscience.iop.org/0953-8984/25/2/025502>)

View [the table of contents for this issue](#), or go to the [journal homepage](#) for more

Download details:

IP Address: 141.219.155.120

The article was downloaded on 03/12/2012 at 16:48

Please note that [terms and conditions apply](#).

First-principles computation of structural, elastic and magnetic properties of Ni₂FeGa across the martensitic transformation

Munima B Sahariah¹, Subhradip Ghosh², Chabungbam S Singh^{1,3}, S Gowtham⁴ and Ravindra Pandey⁴

¹ Institute of Advanced Study in Science and Technology, Guwahati-781035, India

² Indian Institute of Technology Guwahati, Guwahati-781039, India

³ Gauhati University, Guwahati-781014, India

⁴ Michigan Technological University, Michigan 49931-1295, USA

E-mail: munima@iasst.gov.in and munimab@gmail.com

Received 25 July 2012, in final form 12 November 2012

Published 28 November 2012

Online at stacks.iop.org/JPhysCM/25/025502

Abstract

The structural stabilities, elastic, electronic and magnetic properties of the Heusler-type shape memory alloy Ni₂FeGa are calculated using density functional theory. The volume conserving tetragonal distortion of the austenite Ni₂FeGa find an energy minimum at $c/a = 1.33$. Metastable behaviour of the high temperature cubic austenite phase is predicted due to elastic softening in the [110] direction. Calculations of the total and partial magnetic moments show a dominant contribution from Fe atoms of the alloy. The calculated density of states shows a depression in the minority spin channel of the cubic Ni₂FeGa just above the Fermi level which gets partially filled up in the tetragonal phase. In contrast to Ni₂MnGa, the transition metal spin-down states show partial hybridization in Ni₂FeGa and there is a relatively high electron density of states near the Fermi level in both phases.

(Some figures may appear in colour only in the online journal)

1. Introduction

In recent years, both experimental and theoretical research on magnetic shape memory alloys (MSMA) has gained momentum owing to their multifunctional behaviour for novel applications. Apart from the shape memory effect, MSMA alloys exhibit phenomena like the giant magnetocaloric effect and magnetoresistance which are also of technological importance. Ni₂MnGa is one such MSMA which has been studied extensively [1–5]. In spite of its remarkable properties, Ni₂MnGa is found to suffer from some drawbacks such as relatively low Curie and martensitic transformation temperatures, high brittleness, etc. Alternatively, NiFeGa and CoNiGa alloys with compositions close to the stoichiometric Heusler structure have been proposed as promising ferromagnetic shape memory alloys [6, 7]. It is due

to the fact that NiFeGa and CoNiGa alloys have a martensitic transformation domain close to room temperature, which is an essential requirement for technological applications. Moreover there is the possibility of tailoring a dual phase microstructure by including small amounts of the γ phase which increases the ductility of these alloys, and thus opens up a way to overcome the high brittleness of NiMnGa [8]. A detailed investigation of the electronic structure of these new promising alloys is very important for understanding the martensitic transformation mechanisms and other related physical properties. The critical issues related to the martensitic transformation are the changes in the crystallographic and electronic structures. Though these issues have had extensive theoretical study for Co–Ni–Ga alloys [9–12], not much attention has been paid to Ni–Fe–Ga systems except in the works of Liu *et al* [13],

Bai *et al* [14] and Qawasmeh and Hamad [15]. Employing a full-potential linearized-augmented plane-wave (FP-LAPW) method, Liu *et al* [13] considered the martensitic phase to be orthorhombic in structure and focused on the electronic and magnetic properties of the system as it undergoes the martensitic transformation. While Liu *et al* explained the martensitic transformation in Ni₂FeGa as occurring by the same mechanism as in Ni₂MnGa, we arrive at a different conclusion. Recently Qawasmeh and Hamad [15] have also adopted the FP-LAPW method to investigate the structural, electronic and magnetic properties of Ni₂FeGa along with a number of other Heusler alloys. Bai *et al* [14] focused on the charge density and electronic structure of the L2₁ phase using pseudopotential methods. However, the cubic to tetragonal martensitic transformation in terms of electronic structure and the elastic stability has not been discussed explicitly in these works. As per experimental findings, the Ni–Fe–Ga alloy has a two way shape memory effect, a Curie temperature of 430 K and a martensitic transformation temperature of 142 K [16] in stoichiometric and as high as ≈271–277 K in some off-stoichiometric compositions [17, 18].

In this work we consider the martensitic phase to be tetragonal in structure according to the experimental results of Li [19] as well as Alvarado [20] and apart from calculating the electronic and magnetic properties of the system we explore the total energy landscape of the lattice while deforming it tetragonally by varying the c/a ratio. The energy landscape gives us an idea about the stability of the system along the so-called Bain path. We also compute the elastic properties of the system in its austenite phase and try to correlate the structural instability with the elastic one. In all the investigations, Ni₂MnGa alloy has been taken as the prototype and the results for Ni₂FeGa are compared with the prototype material.

2. Theoretical details

All the calculations were performed using density functional theory (DFT) [21, 22] as implemented in the QUANTUM-ESPRESSO code⁵, [23]. We employed the generalized gradient approximation (GGA) for the exchange correlation functional in the formulation of Perdew, Burke and Ernzerhof [24]. For the pseudopotentials used, the electronic configurations were Ni(3d⁸4s²), Mn(3d⁶4s¹), Fe(3d⁷4s¹) and Ga(4s²4p¹), respectively. The Kohn–Sham orbitals were described using a plane-wave basis set. An energy cutoff of 60 Ryd was used to truncate the plane-wave expansion of the electronic wavefunctions. The charge-density cutoff was kept at 12 times that of the kinetic energy cutoff of the respective systems and the Methfessel–Paxton smearing size was fixed at 0.02 Ryd. The Brillouin zone integration was performed over a Monkhorst–Pack 12 × 12 × 12 mesh for the four atom and eight atom primitive cell of the cubic and tetragonal phases, respectively. The modelling

parameters yield an energy convergence of 0.0001 Ryd. The Brillouin zone integration was carried out using smearing with Methfessel–Paxton first-order spreading. A denser k -mesh of 20 × 20 × 20 was used for calculations of density of states.

3. Results and discussion

3.1. Structural properties

The Ni₂FeGa alloy synthesized using a melt-spinning technique contains a well defined L2₁ order at room temperature. The experimental lattice parameter is 5.74 Å with a face centred cubic (fcc) unit cell volume of 189 Å³ [25]. Both stoichiometric and off-stoichiometric compounds with compositions close to Ni₂FeGa undergo a first-order structural transition from the cubic austenite to the tetragonal martensite on cooling [19, 20], just like the prototype Ni₂MnGa. The experimentally observed nonmodulated structure is tetragonal with $c/a > 1$. The cubic L2₁ Heusler structure of the austenite phase and the tetragonal L1₀ structure of the martensite phase are shown in figure 1. The optimized lattice parameters along with the net magnetization of respective phases are listed in table 1. We have compared our values with some existing experimental as well as theoretical results. For austenite Ni₂MnGa and Ni₂FeGa, and for martensite Ni₂MnGa the lattice parameters are in good agreement with the experimental as well as previous theoretical ones. As for magnetic moments the disagreement with the existing theoretical results is about 2% for Ni₂MnGa and about 5% for Ni₂FeGa which can be attributed to the different methods and potentials used for the calculations.

3.2. Elastic properties

The elastic constants of the cubic austenite phases of Ni₂MnGa and Ni₂FeGa obtained at the GGA–DFT level of theory are given in table 2. The three independent elastic constants for the cubic austenite phases are determined by imposing three different deformations on the unit cell under equilibrium. One of the elastic moduli is the bulk modulus B and the other two are the shear moduli C' and C_{44} . The bulk modulus B is obtained by using the strain under hydrostatic pressure $e = (\delta, \delta, \delta, 0, 0, 0)$. The tri-axial shear strain $e = (0, 0, 0, \delta, \delta, \delta)$ and volume conserving orthorhombic strain $e = (\delta, \delta, (1 + \delta)^{-2} - 1, 0, 0, 0)$ are applied for the shear moduli C_{44} and C' , respectively [29, 30].

First, we calculate total energies E and E_0 for the strained and the unstrained lattice respectively. The $(E - E_0)/V_0$ values are then plotted as a function of δ , where V_0 is the equilibrium volume. The strain parameter δ is varied from -0.02 to 0.02 in steps of 0.01 . Figure 2 illustrates the total energy as a function of strain for the three distortions for both systems Ni₂MnGa and Ni₂FeGa. The lines in the figures represent the fourth-order polynomial fit to the energy versus strain curve. The elastic constants are then extracted from the second-order coefficient of the fit of their respective data.

In table 2 we give the values of the elastic constants of the cubic austenite phase. An analysis of the existing theoretical

⁵ QUANTUM-ESPRESSO is a community project for high-quality quantum-simulation software based on density functional theory and coordinated by Paolo Giannozzi. See <http://www.quantum-espresso.org> and <http://www.pwscf.org>.

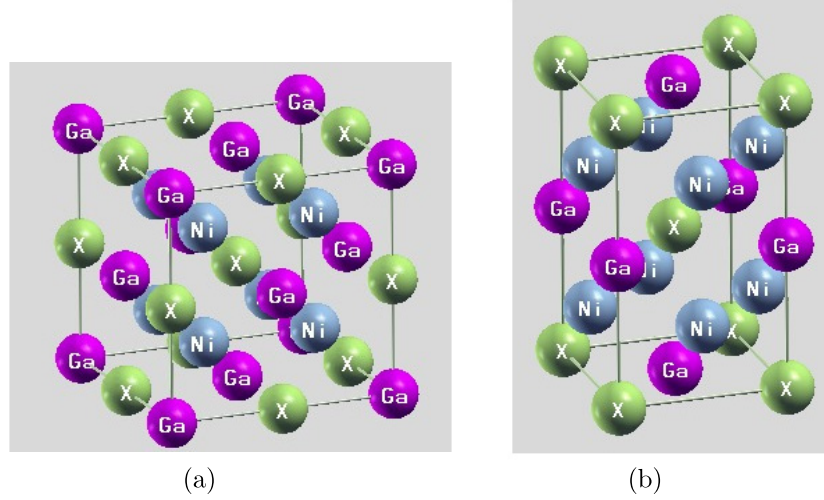


Figure 1. Schematic view of (a) the conventional Heusler structure $L2_1$ in the austenite phase and (b) the tetragonal structure $L1_0$ in the martensite phase.

Table 1. Calculated structural and magnetic parameters of Ni_2MnGa and Ni_2FeGa alloys corresponding to 0 K.

Alloy	Structure	Lattice parameters (Å)	Magnetic moment (μ_B f.u. ⁻¹)
Ni_2MnGa	$L2_1$	$a = 5.81$ (5.82 ^a , 5.81 ^b)	4.17 (4.07 ^b)
	$L1_0$	$a = 5.44$ (5.39 ^b) $c/a = 1.22$ (1.25 ^b)	4.23 (4.14 ^b)
Ni_2FeGa	$L2_1$	$a = 5.77$ (5.74 ^c)	3.31(3.13 ^d)
	$L1_0$	$a = 5.24$ $c/a = 1.33$	3.36

^a Experiment with neutron powder diffraction [26].

^b *Ab initio* calculations by Entel [27].

^c X-ray diffraction (XRD) and Transmission Electron Microscopy (TEM) experiment [25], Single crystal neutron diffraction experiment [28].

^d Full-potential linearized-augmented plane-wave method [13].

Table 2. The bulk modulus B (GPa) and the elastic constants C_{ij} (GPa) of the cubic Ni_2MnGa and Ni_2FeGa alloys.

Alloy	B	C'	C_{11}	C_{12}	C_{44}
Ni_2MnGa	152.7	1.3	154.4	151.8	109.0
Ni_2FeGa	164.4	-1.6	162.2	165.5	103.8

and experimental results for Ni_2MnGa [29, 31–33] reveals that the bulk modulus B and shear moduli C' , C_{44} lie in the range 146–155, 2.5–6.1 and 100–110 GPa, respectively. Except for C' , the calculated values of B and C_{44} are in good agreement with the previously reported results. For Ni_2FeGa , the elastic constant values extracted from the phonon dispersion relations produced by inelastic neutron diffraction experiments gives $C_{11} \approx 163$ GPa, $C_{44} \approx 86$ GPa and $C' \approx 13$ GPa [28]. The experiment was performed at a temperature of 300 K. Our calculated value of C_{11} is in very good agreement with the existing data. Here we note that a complete softening of C' , which corresponds to the long wavelength limit of the TA_2 -phonon branch of the lattice, is predicted at the GGA–DFT level of theory.

We now discuss the stability of the $L2_1$ austenite phase of Ni_2FeGa with respect to the volume conserving tetragonal

distortion. We will also compare the result with that of Ni_2MnGa where the minimum along the so-called Bain path occurs at $c/a \approx 1.22$ in agreement with the previously reported result [34]. Figure 3 shows variation of the energy difference with respect to the minimum energy with c/a for Ni_2MnGa and Ni_2FeGa . We notice that the minimum in energy is predicted to be at $c/a = 1.33$ for Ni_2FeGa , and the E versus c/a curve is essentially flat at $c/a = 1$. At this point, there exists a qualitative difference between the two systems concerned. Unlike Ni_2MnGa , there is no significant local maximum along the transformation path from cubic to tetragonal for Ni_2FeGa . This is a behaviour similar to that of Co_2NiGa , with which the present system shares a number of common physical properties like high Curie temperature, two way shape memory effect etc. There is another point worth discussing regarding the energy versus c/a plots. As shown in the figure, the plot corresponding to Ni_2MnGa is comparatively flatter than that of Ni_2FeGa . This raises concern because this predicts reverse estimates for martensitic transformation temperatures as compared to the experimental values. In fact the experimental samples used for determining the martensitic transformation temperature of Ni_2FeGa had an embedded second phase of off-stoichiometric

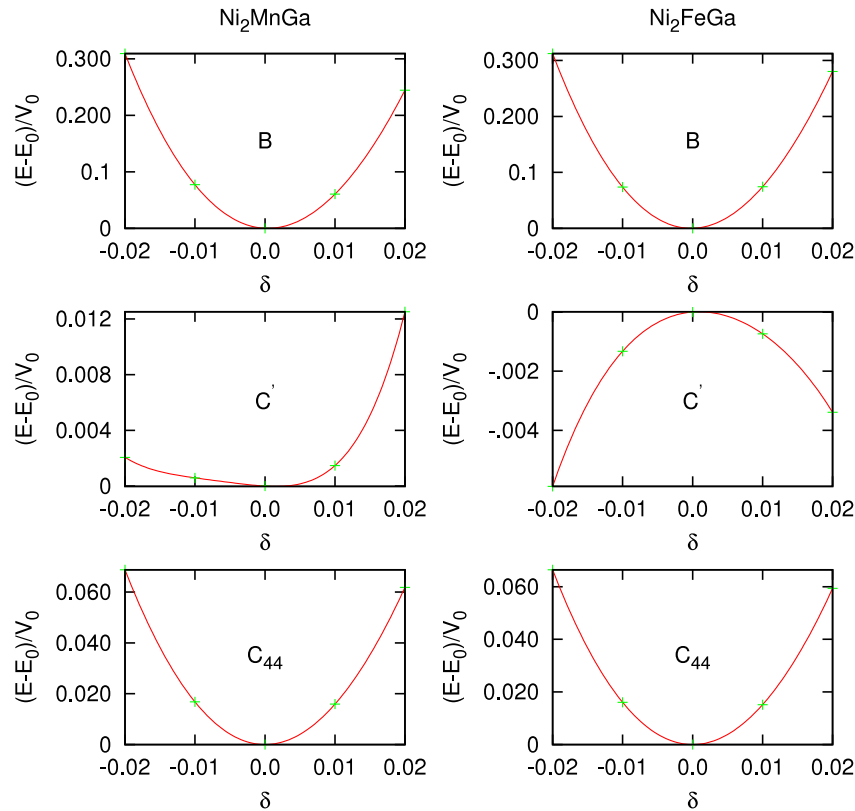


Figure 2. Total energy as a function of strain for Ni₂MnGa and Ni₂FeGa in cubic L₂₁.

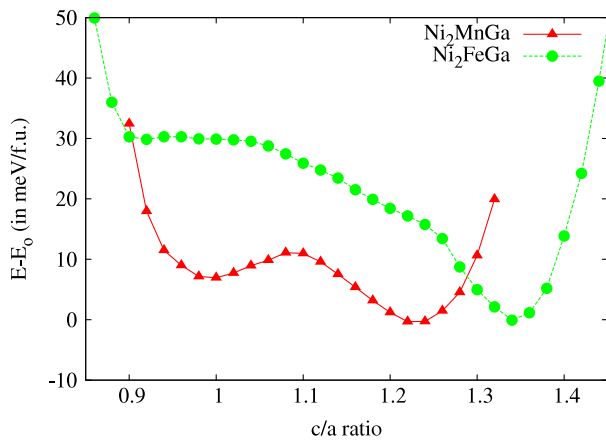


Figure 3. Total energy dependence of Ni₂MnGa and Ni₂FeGa under the variation in c/a .

composition [16]. On the other hand Pal and Mandal [18] predicted that the martensitic transformation temperature of Ni₂FeGa is very sensitive to the composition. Thus the aforementioned anomaly regarding the estimation of martensitic transformation temperature could be attributed to the deviation of the experimental sample from the stoichiometric composition. Further experimental attempts are required to solve this issue.

3.3. Magnetic properties

A detailed analysis of the magnetic moments can provide useful information about the electronic structure of a

magnetic system. Here we investigate the overall change in magnetization of the systems as they undergo a transformation from the cubic austenite phase to the tetragonal martensite phase.

In both the cases, the magnetization increases as the system goes from a higher symmetry to a lower symmetry structure. Similar to Mn of the prototype Ni₂MnGa, Fe has the largest moment of 2.87 and 2.75 μ_B for the austenite and the martensite phases, respectively. As for the Ni sites the magnetic moment increases from 0.2877 to 0.3698 μ_B when the system goes from a high temperature to a low temperature phase. Thus the ferromagnetism primarily originates from the Fe sites. There is a transfer of magnetic moment from Fe to Ni during the martensitic transformation. The contribution from the Ga sites in both systems is small but finite. For a number of Fe based Heusler alloys of type X_2YZ , the full-potential calculations [35] reported that Fe occupying the Y site carries a magnetic moment of the order of 2.7–2.8 μ_B f.u.⁻¹, while the value gets modified to 2.20–2.26 μ_B f.u.⁻¹ when Fe occupies the X site. Table 1 shows an overall decrease in magnetic moment as Mn is substituted by Fe in the lattice. Since contributions from Ni to the total magnetic moment in both cases are small, it is the lower magnetic moment value of Fe which is responsible for the overall reduction of magnetic moments in Ni₂FeGa.

3.4. Electronic structure

Figure 4 shows the total as well as the site-projected d-bands for the austenite phases. As a normal practice, the Fermi levels

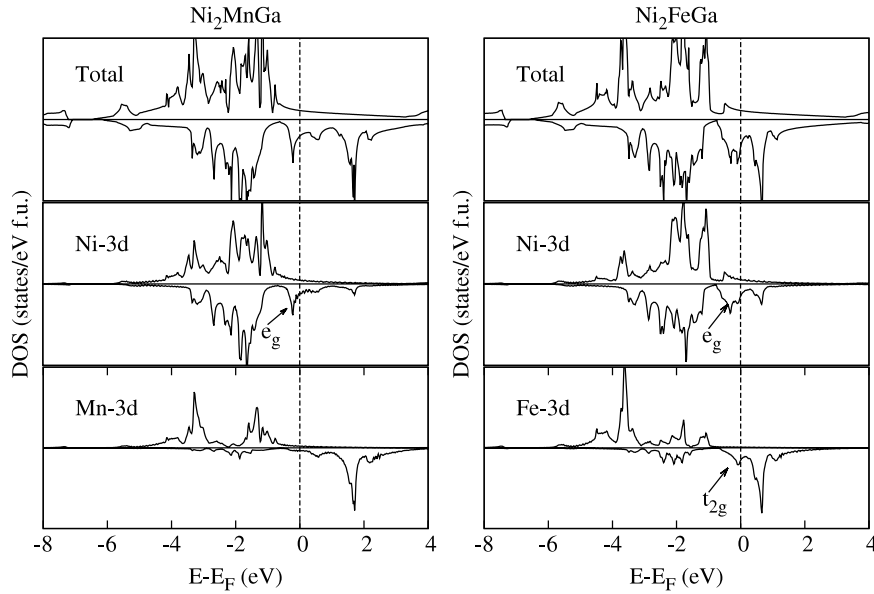


Figure 4. The top left and right panels show the total electronic structure of L2₁ Ni₂MnGa and Ni₂FeGa, respectively. The middle and lower panels show the site-projected d-bands for the transition metal components. The vertical dotted line represents the Fermi level.

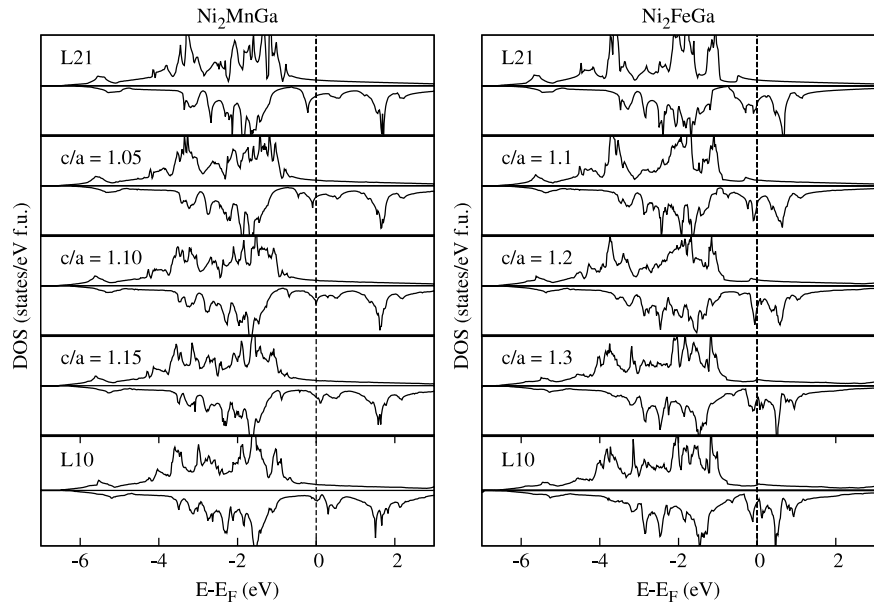


Figure 5. The total electronic DOS for Ni₂MnGa (left) and Ni₂FeGa (right) along the Bain path. The vertical dotted line represents the Fermi level.

are indicated by dotted vertical lines. It is clear from the figure that the qualitative difference in the electronic structure for both systems comes in the minority spin states. Like most of the Heusler alloys, including Ni₂MnGa, a pseudogap is formed in Ni₂FeGa at approximately 1 eV below the Fermi level. Unlike Ni₂MnGa, where the Fermi level sits midway in the valley formed by the bonding and anti-bonding spin-down states, the Fermi level of Ni₂FeGa sits just at the beginning of the valley. The underlying fcc symmetry of the structures give rise to e_g and t_{2g} states in both systems. The dual peak immediately below the Fermi level of Ni₂FeGa comprises Ni- e_g states and Fe- t_{2g} states. On the other hand the large peak above the Fermi level comprises Ni- t_{2g} states and Fe- e_g states.

In the case of Ni₂MnGa there is no sign of hybridization of Ni-3d spin-down states with Mn-3d spin-down states, the respective peaks lying distinctly on either side of the Fermi level. However, the situation is not so extreme in the case of Ni₂FeGa, and we observe that Ni-3d-states hybridize partially with Fe-3d ones for spin-down anti-bonding states.

The characteristic changes of the electronic DOS for both Ni₂MnGa and Ni₂FeGa are now discussed through figure 5 as the systems go from the cubic L2₁ phase to the tetragonal L1₀ phase along the Bain path. The band Jahn–Teller effect is the most common interpretation of the martensitic transformation in Ni₂MnGa which originates from a redistribution of Ni- e_g states forming a peak in minority DOS in the austenite phase.

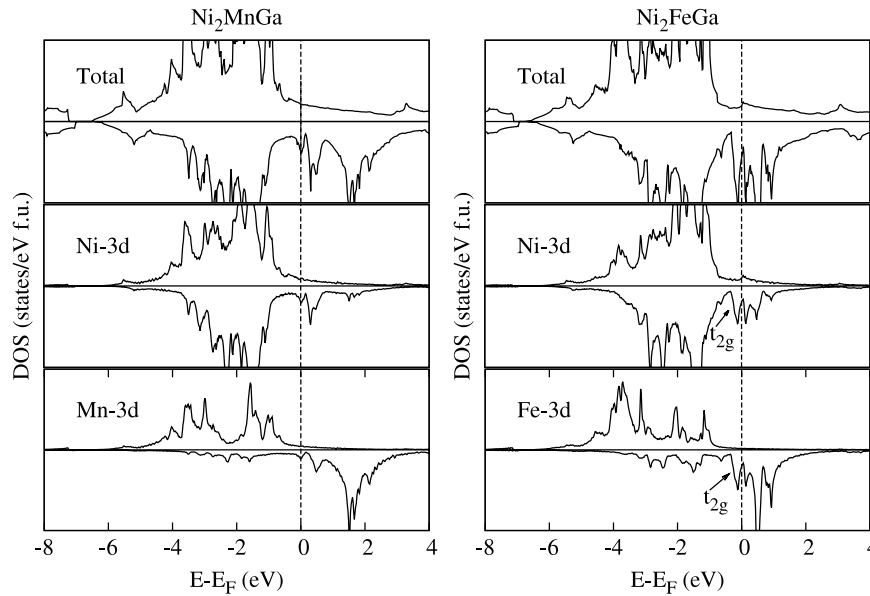


Figure 6. The top left and right panels show the total electronic structure of $L1_0$ Ni_2MnGa and Ni_2FeGa , respectively. The middle and lower panels show the site-projected d-bands for the transition metal components. The vertical dotted line represents the Fermi level.

With tetragonal distortion the Ni- e_g peak gets split into two and one peak diminishes gradually. This has the effect of lowering the energy of the system and thus stabilizing the martensitic phase. The mechanism is somewhat different in Ni_2FeGa . Here the Ni- e_g and Fe- t_{2g} states converges and then split again to form two t_{2g} hybridized states, one just below the Fermi level and another just above it. This also results in a lowering of energy as t_{2g} states are lower in energy compared to e_g . The overall effect is to create an equivalent number of occupied and unoccupied states close to the Fermi level, making the situation distinct from that of Ni_2MnGa .

Figure 6 shows the total as well as the site-projected d-bands for the martensite phases. Just like in austenite phases, here also there is an absence of hybridization of 3d-states in the case of Ni_2MnGa and weak hybridization in the case of Ni_2FeGa .

4. Conclusions

We have studied the structural stabilities of the Ni_2FeGa alloy by looking at the energy landscape along the tetragonal distortion path of the Heusler structure and by computing the elastic constants in the cubic Heusler phase at 0 K. We predict a metastable behaviour of the high temperature cubic austenite phase which can be correlated to elastic softening in the [110] direction. The energy landscape does not exhibit any local maxima along the transformation path. Calculations of the total and partial magnetic moments show that Ni_2FeGa has an overall lower value of magnetic moment in both phases as compared to that of Ni_2MnGa . An analysis of the individual atomic contributions reveals that it is the Fe which lowers the overall magnetization of the system. There are two possible ways we can raise the magnetization as well as the martensitic transformation temperature—by changing the composition of various constituents or by alloying Fe

with some other transition metal like Co. a few experiments have already successfully explored the first possibility [17, 18]. In both systems, the majority spin states are occupied and hence do not play any part in stabilizing the martensitic phase. As far as the minority spin states are concerned there is a qualitative difference in their behaviour for both systems over the martensitic transformation. In the case of Ni_2MnGa it is the so-called band Jahn–Teller mechanism which stabilizes the martensitic phase, whereas in case of Ni_2FeGa the stabilization occurs by virtue of the shifting of occupations from e_g states to the low lying t_{2g} states. In accordance with the previous results, we find that there is no hybridization amongst the 3d-transition metal states in Ni_2MnGa . On the other hand the 3d-states of Ni and Fe in Ni_2FeGa show partial hybridization. Unlike Ni_2MnGa there is high density of electronic states just below and above the Fermi level of Ni_2FeGa . This relatively high electron density of states around the Fermi level in both phases indicates that it will be interesting to study the Fermi surface topology for an understanding of the structural transformation.

Acknowledgments

MBS and CSS acknowledge support from IIT Guwahati and Michigan Tech University in terms of computational facilities.

References

- [1] Gruner M E, Adeagbo W A, Zayak A T, Hucht A, Buschmann S and Entel P 2008 *Eur. Phys. J. Spec. Top.* **158** 193
- [2] Hu Q-M, Li C-M, Yang R, Kulkova S E, Bazhanov D I, Johansson B and Vitos L 2009 *Phys. Rev. B* **79** 144112
- [3] Uijttewaaij M A, Hickel T, Neugebauer J, Gruner M E and Entel P 2009 *Phys. Rev. Lett.* **102** 035702
- [4] Buchelnikov V D, Sokolovskiy V V, Taskaev S V, Khovaylo V V, Aliev A A, Khanov L N, Batdalov A B,

- Entel P, Miki H and Takagi T 2011 *J. Phys. D: Appl. Phys.* **44** 064012
- [5] Ghosh S, Vitos L and Sanyal B 2011 *Physica B* **406** 2240
- [6] Dogan E et al 2011 *Acta Mater.* **59** 1168
- [7] Zhang H R and Wu G H 2011 *Acta Mater.* **59** 1249
- [8] Font J et al 2008 *Mater. Sci. Eng. A* **481/482** 262
- [9] Arroyave R, Junkaew A, Chivukula A, Bajaj S, Yao C-Y and Garay A 2010 *Acta Mater.* **58** 5220
- [10] Siewert M, Gruner M E, Dannenberg A, Hucht A, Shapiro S M, Xu G, Schlagel D L, Lograsso T A and Entel P 2010 *Acta Mater.* **58** 5220
- [11] Singh N, Dogan E, Karaman I and Arroyave R 2011 *Phys. Rev. B* **84** 184201
- [12] Dai X, Liu G, Li Y, Qu J, Li J, Chen J and Wu G 2007 *J. Appl. Phys.* **101** 09N503
- [13] Liu Z H, Hu H N, Liu G D, Cui Y T, Zhang M, Chen J L and Wu G H 2004 *Phys. Rev. B* **69** 134415
- [14] Bai J, Raulot J M, Zhang Y D, Esling C, Zhao X and Zuo L 2011 *J. Appl. Phys.* **109** 014908
- [15] Qawasmeh Y and Hamad B 2012 *J. Appl. Phys.* **111** 033905
- [16] Liu Z H, Zhang M, Cui Y T, Zhou Y Q, Wang W H, Wu G H, Zhang X X and Xiao G 2003 *Appl. Phys. Lett.* **82** 424
- [17] Hamilton R F, Efstathiou C, Sehitoglu H and Chumlyakov Y 2006 *Scr. Mater.* **54** 465
- [18] Pal D and Mandal K 2010 *J. Phys. D: Appl. Phys.* **43** 455002
- [19] Li Y, Jiang C, Liang T, Ma Y and Xu H 2003 *Scr. Mater.* **48** 1255
- [20] Alvarado-Hernandez E, Soto-Parra D E, Ochoa-Gamboa R, Castillo villa P O, Flores-Zuniga H and Rios-Jara D 2008 *J. Alloys Compounds* **462** 442
- [21] Hohenburg P and Kohn W 1964 *Phys. Rev. B* **136** 864
- [22] Kohn W and Sham L J 1965 *Phys. Rev.* **140** A1133
- [23] Scandolo S and Giannozzi P et al 2005 *Z. Kristallogr.* **220** 574
- [24] Perdew J P, Burke K and Ernzerhot M 1996 *Phys. Rev. Lett.* **77** 3865
- [25] Du Z W, Shao B L, Liu A S, Wu G H, Qian J F, Zhang Z Y and Gao Z 2011 *J. Mater. Sci.* **46** 2733
- [26] Brown P J, Crangle J, Kanomata T, Matsumoto M, Neumann K-U, Ouladdiaf B and Ziebeck K R A 2002 *J. Phys.: Condens. Matter* **14** 10159
- [27] Entel P, Dannenberg A, Siewert M, Herper H C, Gruner M E, Comtesse D, Elmers H-J and Kallmayer M 2011 *Metall. Mater. Trans. A* doi:10.1007/s11661-011-0832-7
- [28] Perez-Landazabal J I, Recarte V and Sanchez-Alarcos V 2009 *Phys. Rev. B* **80** 144301
- [29] Kart S O and Cagin T 2010 *J. Alloys Compounds* **508** 177
- [30] Wang S Q and Ye H Q 2003 *J. Phys.: Condens. Matter* **15** 5307
- [31] Worgull J, Petti E and Trivisonno J 1996 *Phys. Rev. B* **54** 15695
- [32] Bungaro C, Robe K M and Dal Corso A 2003 *Phys. Rev. B* **68** 134104
- [33] Kart S O, Uludogan M, Karaman I and Cagin T 2007 *Phys. Status Solidi a* **205** 1026
- [34] Entel P, Buchelnikov V D, Khovailo V V, Zayak A T, Adeagbo W A, Gruner M E, Herper H E and Wassermann E F 2006 *J. Phys. D: Appl. Phys.* **39** 865
- [35] Kulkova S E, Eremeev S V, Kakeshita T, Kulkov S S and Rudenski G E 2006 *Mater. Trans.* **47** 599